Engineering Structures 199 (2019) 109597

Contents lists available at ScienceDirect

Engineering Structures

journal homepage: www.elsevier.com/locate/engstruct

A new stochastic formulation for synthetic hurricane simulation over the North Atlantic Ocean

Wei Cui[a,b,c,d], Luca Caracoglia[b,*]

[a] State Key Lab of Disaster Reduction in Civil Engineering, Tongji University, Shanghai 200092, China
[b] Department of Civil and Environmental Engineering, Northeastern University, Boston, MA 02115, USA
[c] Department of Bridge Engineering, College of Civil Engineering, Tongji University, Shanghai 200092, China
[d] Key Laboratory of Transport Industry of Bridge Wind Resistance Technologies, Tongji University, Shanghai 200092, China

ARTICLE INFO

Keywords:
Hurricane hazard
Hurricane track
Hurricane frequency
Wind speed
Performance-based wind engineering

ABSTRACT

Hurricanes are among the most destructive weather phenomena in the United States (US) of America. Accurate modeling of hurricane trajectories, as they land ashore and approach the built environment, is important for public safety. This study presents a new stochastic model for the simulation of hurricane trajectories in the North Atlantic Ocean. Trajectory of the hurricane eye is modeled as a two-dimensional partially-correlated Brownian motion with drift term. Hurricane intensity is modeled as a second-order auto-regressive process, accounting for sea surface temperature.

The model is validated by comparing the numerically-generated hurricane tracks against historical records, derived from the HurDat database (NOAA, National Oceanic and Atmospheric Administration). Simulated hurricane arrival and landing rates along the US Eastern coastline are also examined to demonstrate model validity. Finally, performance-based wind engineering (PBWE) application is presented by comparing simulated hurricane wind speeds against ASCE 7-16 recommendations.

1. Introduction

Hurricanes are among the most destructive weather phenomena, which can cause severe damage to properties and loss of life due to strong winds and surge effects. In 2005, Hurricane Katrina caused 1833 fatalities and 108 billion USD property damage along the coast of the Gulf of Mexico. In 2012, Hurricane Sandy led to about 65 billion USD damage in the northeastern coastal region of the USA and even in the Ontario Province of Canada, which are usually not considered hurricane-prone areas. As a result, the severity of hurricane threat has motivated several studies, aiming to accurately forecast hurricane activity in both near and distant future. A short review of the most important models, currently employed for hurricane simulation in wind engineering, is provided in the following.

Georgiou first introduced a pioneering method to numerically model the hurricane wind field and to predict hurricane wind speed along the US Atlantic coastline [1]. *Simiu* proposed a "single-site" probabilistic model, using Monte Carlo simulation method, to compute hurricane wind speed as a function of five random quantities or parameters [2,3]. Subsequently, *Vickery* proposed an empirical hurricane track model [4,5], derived from linear statistical regression of a large hurricane database. This model has been comprehensively validated and widely used in civil engineering for long-term hurricane predictions; this seminal work led to many subsequent studies on hurricane wind speed forecast [6–9].

Currently, the Vickery's method [4] is the most widely used approach for hurricane hazard simulation. For instance, the ASCE 7 design standard has adopted this model to provide the basic design wind speed in hurricane-prone regions of the USA and the wind hazard maps [10]. Based on Vickery's pioneering hurricane model, several researchers have made further contributions to various application fields. For example, Vickery's method has been adapted to other Ocean regions and to predict typhoon wind speeds along the northwestern Pacific coast of Asia [11]. This method has also be used to examine the potential influence of "climate change" on hurricane activities [12,13] and consequent effects on structural integrity and damage probability to buildings [14].

However, recent studies have indicated [14] that Vickery's model parameters are, on occasion, difficult to determine by regression analysis due to a number of initial assumptions that are implicitly

* Corresponding author at: Department of Civil and Environmental Engineering, Northeastern University, 400 Snell Engineering Center, 360 Huntington Avenue, Boston, MA 02115, USA.
E-mail address: lucac@coe.neu.edu (L. Caracoglia).

https://doi.org/10.1016/j.engstruct.2019.109597
Received 4 August 2018; Received in revised form 26 July 2019; Accepted 27 August 2019
Available online 09 September 2019
0141-0296/

embedded in the original model [4]. As a result, synthetically replicating the hurricane trajectories may be challenging. In this study, an alternative formulation is explored to simulate hurricane trajectories and hurricane intensity, which can achieve results comparable to Vickery's method by limiting the number of initial assumptions.

2. Vickery's empirical storm track model: review and study motivation

2.1. Track-model equations

Vickery's model [4] is based on the following equations [Eqs. (1) and Eq. (2) below], which can be used to synthetically generate a sample of hurricane tracks:

$$\Delta \ln c_{i+1} = a_1 + a_2\psi + a_3\lambda + a_4 \ln c_i + a_5\theta_i + \epsilon_c \tag{1a}$$

$$\Delta\theta_{i+1} = b_1 + b_2\psi + b_3\lambda + b_4 c_i + b_5\theta_i + b_6\theta_{i-1} + \epsilon_\theta \tag{1b}$$

$$\ln(I_{i+1}) = c_0 + c_1\ln(I_i) + c_2\ln(I_{i-1}) + c_3\ln(I_{i-2}) + c_4 T_{si} + c_5(\Delta T_s) + \epsilon_I \tag{2}$$

In Eq. (1a) and in Eq. (1b), respectively, $a_j (j = 1, 2\cdots5)$ and $b_j (j = 1, 2\cdots6)$ are coefficients that can be found by linear regression. The quantities ψ and λ are latitude and longitude of the hurricane eye position, c_i is hurricane translation speed at time step i;θ_i is the hurricane heading (direction) at time step i and θ_{i-1} is the hurricane heading at time step $i-1$. When hurricane heading is North, $\theta = 0$, and the limits of θ are $-180 < \theta \leq 180$.

In Eq. (2), the relative intensity I [15] (defined at various time steps i, $i-1$, etc.) is used as a non-dimensional term that relates the actual hurricane pressure deficit Δp to the greatest possible central pressure deficit allowed by the "average climatology" of the hurricane season [4]. ΔT_s is the SST (sea surface temperature) difference between time step i and time step $i+1$, which is calculated as $\Delta T_s = T_{si+1} - T_{si}$. Introducing SST into the model reduces some of the unexplained variability in the central pressure modeling [4]. The variations of heading and translation velocity between time step i and time step $i+1$ are calculated from $\Delta\theta$ and $\Delta \ln c$.

All the coefficients of the model equations in Eqs. (1) and (2) can be estimated by linear regression [4], using a database of historical track records (HurDat) that is maintained in by the National Oceanic and Atmospheric Administration (NOAA). The coefficients are independently derived for each rectangular non-overlapping cell of extension $5^\circ \times 5^\circ$, subdividing the Atlantic Ocean region [4]. Moreover, the coefficients are different for east-heading and west-heading hurricanes. For the cells with insufficient historical data, the coefficients of a nearby cell can be used during hurricane simulation. The quantities ϵ_c, ϵ_θ and ϵ_I are linear regression residuals in Eq. (1a), Eq. (1b) and Eq. (2), respectively. More discussion on ϵ_c, ϵ_θ and ϵ_I is presented in a subsequent section.

2.2. Decay model

Once a hurricane lands on the continent, the hurricane can no longer accumulate energy since the power source (sea) has been cut off. The friction between the hurricane system and the ground (land) reduces the hurricane strength. Consequently, the decay of hurricane intensity after landing needs to be modeled; this model, in its simplest form, is [4]:

$$\Delta p(t) = \Delta p_0 \cdot \exp(-a t_h) \tag{3}$$

The quantity $\Delta p(t)$ is the hurricane central pressure deficit at time t_h (in hours) after landing. The quantity Δp_0 is the hurricane central pressure deficit at initial landing time ($t = 0$). The parameter a is an exponential decay rate over time t_h.

As explained by Vickery and Twisdale [16], a is a site-specific coefficient which can be related to central pressure deficit Δp as:

Table 1
Exponential decay rate for different sites - reproduced from [16].

Region	a_0	a_1	σ_{ϵ_a}
Florida Peninsula	0.006	0.00046	0.0025
Gulf-of-Mexico Coast	0.035	0.00050	0.0355
Atlantic Coast	0.038	0.00029	0.0093

$$a = a_0 + a_1\Delta p + \epsilon_a \tag{4}$$

The term ϵ_a is a linear regression residual, which can be modeled as a normal random variable with zero mean. The model for the simulation of hurricane decay intensity, presented in [16], is used in this study. Even though several model updates are available in Eqs. (3) and (4) [e.g. 17], the original model has been widely used by researchers to simulate hurricane decay and it is believed to be acceptable for the purposes of this comparative study, since it enables other researches to replicate the simulations if desired.

The a_0, a_1 and the standard deviation σ_{ϵ_a} of ϵ_a are shown in Table 1.

2.3. Georgiou's gradient wind field model

When a hurricane approaches the continent, it is necessary to estimate the hurricane wind field in order to compute the hurricane's effect on structures. The actual hurricane wind field can usually be obtained by aircraft reconnaissance observations. Aircraft typically record wind speeds at an elevation of 3000 m, higher than the gradient-level wind speed, which usually occurs between 500 m and 2000 m above the ground surface [18]. Mature hurricane gradient wind fields can be simplified as a large vortex accompanied by a translation motion. Therefore, the gradient wind speed, V_g, can be decomposed into a rotational component, V_R, and a translation component, V_T, as shown in Fig. 1.

The rotational component V_R is assumed to be radially symmetrical about the hurricane eye; the magnitude can be described as a function of the distance r from the hurricane eye. The translation speed can be found from Eq. (1) in the track simulation. The gradient wind speed, using vector summation between rotational wind speed and translation speed, can be determined as described in Georgiou's model [1]:

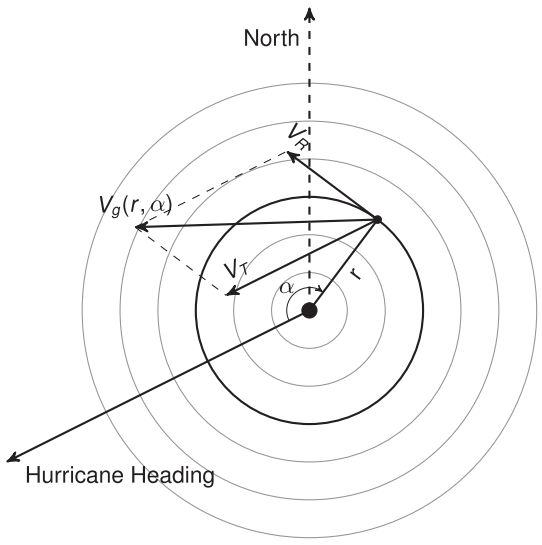

Fig. 1. Hurricane wind field and resultant gradient wind speed.

$$V_g = \frac{1}{2}\left(c\sin\alpha - fr\right) + \sqrt{\frac{1}{4}(c\sin\alpha - fr)^2 + \frac{100B\Delta p}{\rho}\left(\frac{R_{\max}}{r}\right)^B \exp\left[-\left(\frac{R_{\max}}{r}\right)^B\right]} \quad (5)$$

In Eq. (5) c is the magnitude of the translation speed, α is the relative angle between the hurricane heading and radial position, $R_{\max}$ is the radial distance from hurricane eye corresponding to maximum winds; $R_{\max}$ is calculated from [7]:

$$\ln R_{ax} = 2.63 - 0.000508(\Delta p)^2 + 0.0394\psi + \epsilon_R \quad (6)$$

in which ϵ_R is a normal random variable $N(0, 0.40)$ for all latitudes.

The Holland parameter B in Eq. (5) is modeled as:

$$B = 1.38 + 0.00184\Delta p - 0.00309R_{\max} \quad (7)$$

In the previous equations the quantities are expressed as: $R_{\max}$ and r in kilometers, Δp in millibar, air density ρ in kg/m^3; f is the Coriolis parameter in s^{-1}.

2.4. Supplementary examination of Vickery's method and study objectives

By reviewing Vickery's method described above, it must be acknowledged that the three data-driven hurricane simulation equations, Eqs. (1) and (2), may not be sufficient to achieve the simulation accuracy demonstrated in [4].

The following adjustments or refinements must be incorporated into Vickery's hurricane model:

- two sets of parameters in Eqs. (1) and (2) are required for east-heading and west-heading hurricanes;
- refinement of the longitude-latitude grid subdivision may be needed once more hurricane data become available close to coastline regions;
- additional local modifications to the parameters may be necessary to improve hurricane model predictions for various coastal regions.

However, the general public has limited access to some useful information about grid refinement and parameter adjustment. It is on occasion challenging for other researchers to simulate hurricanes by replicating Vickery's method. For these reasons, an alternative, novel approach, based on stochastic processes and inspired by Vickery's method, is proposed in the next section.

3. Proposed hurricane tracking model based on Brownian motion

3.1. Simplification of Vickery's method

Further examination of the regression coefficients in Eqs. (1) and (2) is performed. A detailed analysis of the historical hurricane database using Vickery's method has revealed that the overall correlation among the variables in Eq. (1) can be small. For example, Table 2 presents the Pearson linear correlation among the coefficients in Eq. (1). Regression data, used to determine the coefficients, are extracted from all historical hurricanes crossing the grid cell (80–75°W, 25–30°N).

Table 2
Pearson linear correlation among regression coefficients in Eq. (1).

	ψ	λ	c_i
$\Delta\ln c_{i+1}$	0.0146	0.0028	−0.0626
$\Delta\theta_{i+1}$	0.0401	−0.0222	−0.0216
	$\ln c_i$	θ_i	θ_{i-1}
$\Delta\ln c_{i+1}$	−0.1516	0.0334	−0.0260
$\Delta\theta_{i+1}$	0.0011	−0.3092	−0.2619

The information in Table 2 suggests that both $\Delta\ln c_{i+1}$ and $\Delta\theta_{i+1}$ variables have very small correlation in comparison with geographic coordinates ψ and λ, and the correlation between translation speeds $\ln c_i$ and direction θ_i is also limited. The correlation can be seen between each variable pair either at the current time step i or immediately preceding time steps. The correlation coefficients of $\Delta\ln c_{i+1}$ and $\Delta\theta_{i+1}$ between the other variables are all below 0.07.

After eliminating the nearly uncorrelated terms, Eq. (1) can be simplified to:

$$\Delta\ln c_{i+1} = a_1 + a_4\ln c_i + \epsilon_c \quad (8a)$$

$$\Delta\theta_{i+1} = b_1 + b_5\theta_i + b_6\theta_{i-1} + \epsilon_\theta \quad (8b)$$

The previous equation and observations suggest that both c_i and θ_i only depend on their previous state. Thus Eq. (1) is reduced to a Markov-chain model. It is plausible to simulate these variables, and consequently the hurricane tracks, through Brownian Motion models by eliminating the dependency on some of the variables. The current hurricane location can be simply related to the location at the previous time step. Moreover, Eq. (1) is based on polar coordinates, requiring all the coefficients a_i and b_i to be different for west-heading and east-heading hurricanes due to the Coriolis effect [4]. This complication may be alleviated by converting the original model to Cartesian (planar) coordinates. It is also useful to represent the model in terms of stochastic differential equations [19] and as a Markov-chain model.

$$\begin{bmatrix} dU \\ dV \end{bmatrix} = \begin{bmatrix} \mu_u(\psi,\lambda) \\ \mu_v(\psi,\lambda) \end{bmatrix} dt + \begin{bmatrix} \sigma_u(\psi,\lambda) & \sigma_{uv}(\psi,\lambda) \\ \sigma_{vu}(\psi,\lambda) & \sigma_v(\psi,\lambda) \end{bmatrix} \begin{bmatrix} dW_u \\ dW_v \end{bmatrix} \quad (9)$$

In Eq. (9), the rectangular (Cartesian) components U and V of the hurricane translation speed along longitude (λ) and latitude (ψ) are two-dimensional (2D) correlated Wiener processes as a function of time t. Quantities $\mu_u(\psi,\lambda)$ and $\mu_v(\psi,\lambda)$ are drift terms in the two directions (longitude and latitude, respectively), which represent the hurricane average acceleration components in the two directions. Quantities $\sigma_u(\psi,\lambda)$ and $\sigma_v(\psi,\lambda)$ are diffusion terms, describing the hurricane acceleration randomness in the two directions. The correlation between hurricane motions in the two directions is expressed in terms of "root-covariance" $\sigma_{uv}(\psi,\lambda) = r(\psi,\lambda)\sqrt{\sigma_u(\psi,\lambda)\sigma_v(\psi,\lambda)}$, where $r(\psi,\lambda)$ is the correlation coefficient.

Since Eq. (9) is based on Cartesian coordinates rather than polar coordinates as in Eq. (8), the correlation coefficient $r(\psi,\lambda)$ is introduced to simulate the synchronized hurricane translation changes along both longitude and latitude direction.

W_u and W_v are uncorrelated standard Wiener processes [19]. It should be noted that uncertainty in the hurricane track translation, quantified as ϵ_c and ϵ_θ in [4], is transformed into $\sigma_u(\psi,\lambda)$, $\sigma_v(\psi,\lambda)$ and $r(\psi,\lambda)$ in the new model.

3.2. Verifying hypothesis of Brownian motion for hurricane motion modeling

The Brownian motion theory states that probability distribution of any increment $[U(t+\Delta t) - U(t)]$ exclusively depends on the duration Δt of the time interval (independent increments). This hypothesis can be expressed as follows:

$$\overline{\mu}_{u,\Delta t}(\psi,\lambda) \equiv \int_{\Delta t} \mu_u(\psi,\lambda)dt \propto \Delta t \quad (10a)$$

$$\overline{\mu}_{v,\Delta t}(\psi,\lambda) \equiv \int_{\Delta t} \mu_v(\psi,\lambda)dt \propto \Delta t \quad (10b)$$

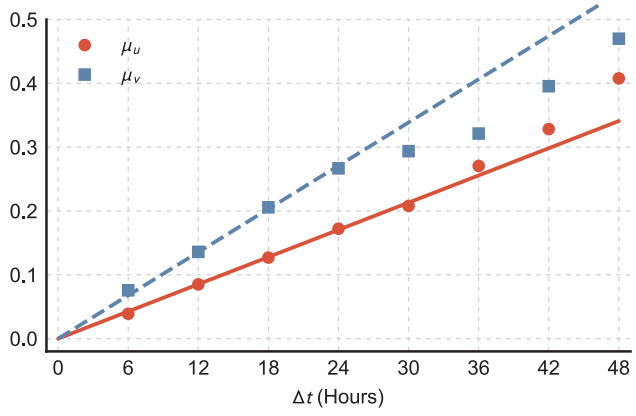

(a) $\overline{\mu}_{u,\Delta t}(\psi,\lambda)$ and $\overline{\mu}_{v,\Delta t}(\psi,\lambda)$

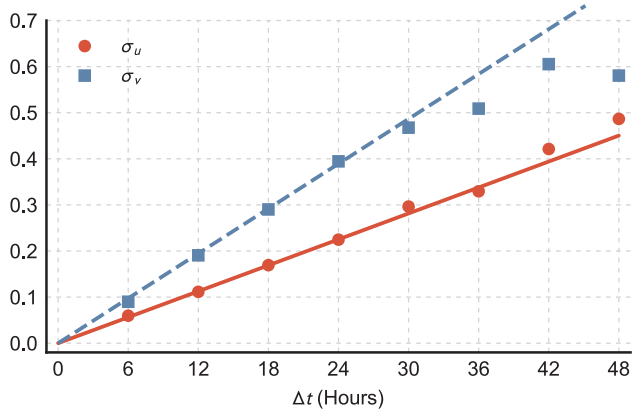

(b) $\overline{\sigma}_{u,\Delta t}(\psi,\lambda)$ and $\overline{\mu}_{v,\Delta t}(\psi,\lambda)$

Fig. 2. Evaluation of Brownian motion independent-increment property (time stationarity) for hurricane track and motion modeling.

$$\overline{\sigma}_{u,\Delta t}\left(\psi,\lambda\right) \equiv \int_{\Delta t} \sigma_u\left(\psi,\lambda\right) \mathrm{d}W_u \propto \Delta t \tag{10c}$$

$$\overline{\sigma}_{v,\Delta t}\left(\psi,\lambda\right) \equiv \int_{\Delta t} \sigma_v\left(\psi,\lambda\right) \mathrm{d}W_v \propto \Delta t \tag{10d}$$

in which $\overline{\mu}_{\Delta t}$ and $\overline{\sigma}_{\Delta t}$ denote the mean and RMS acceleration over time duration Δt respectively. In the previous equations, the integrals are evaluated in accordance with the principles of stochastic calculus [19]. Adequacy of the Brownian motion model to describe hurricane trajectory is evaluated by computing the mean and variance values of hurricane's trajectory acceleration along longitude and latitude at $\Delta t = \{6, 12, 18, 24, 30, 36, 42, 48\}$ hours duration. The results are shown in Fig. 2 for the grid cell N20-25° W65-60°.

From the HurDat hurricane database, all hurricanes entering the cell N20-25° W65-60° are analyzed to derive the average hurricane trajectory acceleration, $\overline{\mu}_{u,\Delta t}(\psi,\lambda)$, $\overline{\mu}_{v,\Delta t}(\psi,\lambda)$, in Fig. 2a and standard deviation of hurricane trajectory acceleration, $\overline{\sigma}_{u,\Delta t}(\psi,\lambda)$, $\overline{\sigma}_{v,\Delta t}(\psi,\lambda)$, in Fig. 2b. Quantities $\overline{\mu}_{u,\Delta t}$, $\overline{\mu}_{v,\Delta t}(\psi,\lambda)$, $\overline{\sigma}_{u,\Delta t}(\psi,\lambda)$ and $\overline{\sigma}_{v,\Delta t}(\psi,\lambda)$ are numerically evaluated at $\Delta t = \{6, 12, 18, 24, 30, 36, 42, 48\}$ hours duration and plotted as markers in Fig. 2. The straight lines in Fig. 2 are from the least square fitting with zero intercept, using the first four data points for $\overline{\mu}_{u,\Delta t}$, $\overline{\mu}_{v,\Delta t}(\psi,\lambda)$, $\overline{\sigma}_{u,\Delta t}(\psi,\lambda)$ and $\overline{\sigma}_{v,\Delta t}(\psi,\lambda)$.

Excellent match can be found between the markers and straight lines in Fig. 2 when $0 < t \leqslant 24$ hours. When $t > 24$ hours, some discrepancy can be found between the fitted lines and data markers due to accumulation of local geographic effects and insufficient data samples. This simulation demonstrates that the hurricane motion can be modeled by Brownian motion using a small time step, e.g. $\Delta t = 6$ hours.

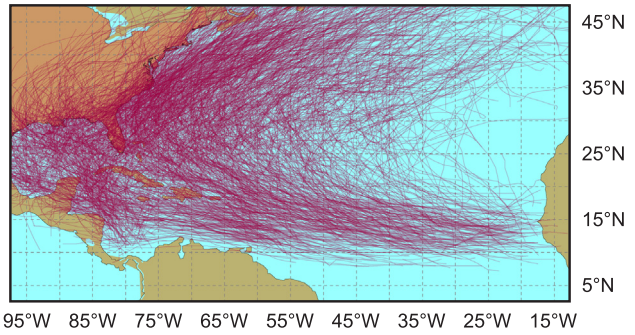

Fig. 3. Hurricane trajectory paths recorded by the North Atlantic Hurricane Database (HurDat).

3.3. Determination of hurricane track model coefficients

Fig. 3 presents the hurricane trajectory paths derived from the North Atlantic Hurricane Database (HurDat). The parameter calibration, as outlined above, is performed on the whole North Atlantic Ocean basin. Following the work by Vickery, the model coefficients are first derived by dividing the Atlantic Ocean region in rectangular non-overlapping cells of extension $5^\circ \times 5^\circ$. In each cell, the hurricane motions are assumed as Brownian motion processes with independent increments. Since the time step length in HurDat is 6 hours, the time step increments employed for coefficient calibration and hurricane modelling will also be 6 hours.

Estimates of $\mu_u(\psi,\lambda)$, $\mu_v(\psi,\lambda)$ are computed by least squares fitting method, and $\sigma_u(\psi,\lambda)$, $\sigma_v(\psi,\lambda)$ and $r(\psi,\lambda)$ are derived from the residuals of the least squares fitting. $\sigma_u(\psi,\lambda)$, $\sigma_v(\psi,\lambda)$ and $r(\psi,\lambda)$ terms are all position dependent. Spatial interpolation [20] is subsequently used to compute the values of the coefficient between adjacent cells. For the cells with insufficient hurricane data, compromising the accuracy of the regression analysis, the coefficients are determined using linear extrapolation from the nearest cells.

Fig. 4 presents the values of the *drift* coefficients $\mu_u(\psi,\lambda)$ and $\mu_v(\psi,\lambda)$ for the entire North Atlantic region. The spatial distribution of $\mu_u(\psi,\lambda)$ is compatible with the hurricane motion trajectories presented in Fig. 3. In Fig. 4a, $\mu_u(\psi,\lambda)$ are slightly smaller than 0, and $\mu_v(\psi,\lambda)$ are slightly greater than 0 for the region with latitudes between 5–15°N and longitude between 65–35°W. This trend indicates that, in the tropical regions, hurricanes tend to move north-west at low translation speeds until they reach an offshore area near the coast. In the intermediate-latitude offshore regions between 15–30°N, both $\mu_u(\psi,\lambda)$ and $\mu_v(\psi,\lambda)$ are greater than 0; consequently, hurricanes tend to veer their heading to northeast and accelerate, thus increasing the translation speeds. In high-latitude offshore regions above 30°N, $\mu_u(\psi,\lambda)$ are greater than 0.4 and $\mu_v(\psi,\lambda)$ are smaller than -0.3; therefore hurricanes tend to decelerate rapidly in the latitude direction. At a later stage, hurricanes are normally dispersed over cold water. The regression results for the *diffusion* parameters $\sigma_u(\psi,\lambda)$, $\sigma_v(\psi,\lambda)$ and $r(\psi,\lambda)$ are plotted in Fig. 5; they follow the same trends as the drift coefficients. The trajectory variability is low at the low latitudes, where most historical data points are available during the first stages of hurricane motion; on the contrary standard deviations and root covariances increase in the regions above 30°N as the hurricanes enter colder regions and data records tend to be sparser.

3.4. Hurricane track model simulation results

Using the coefficients in Figs. 4 and 5 and the hurricane initial position, sampled from historical hurricane records, hurricane tracks can be numerically generated by Eq. (9). As an example, 100 synthetic hurricane tracks are plotted in Fig. 6. Visual inspection against historical hurricane tracks [13] and similar projections provided by other researchers [13,20] indicates that the proposed simulation algorithm is

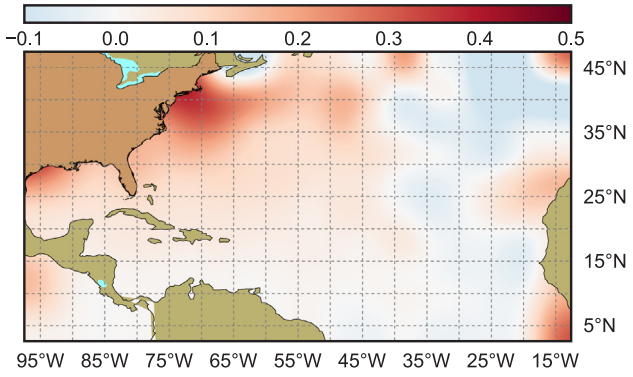

(a) $\mu_u(\psi, \lambda)$

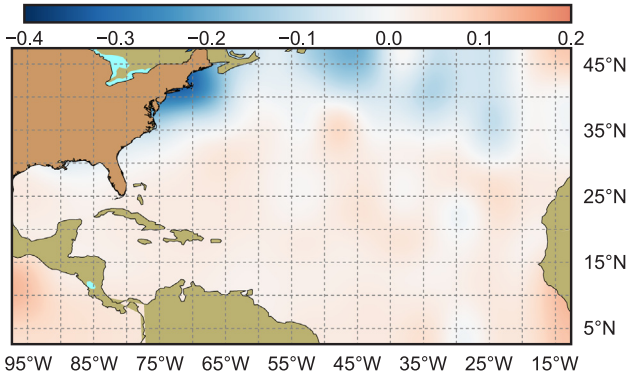

(b) $\mu_v(\psi, \lambda)$

Fig. 4. Spatially-dependent hurricane track model *drift* coefficients.

an effective, simple alternative to Vickery's method. More detailed comparison will be further discussed in Section 5.

The rare events or phenomena, such as hurricane veering, can be simulated through the cases with sequential extreme values of $(\epsilon_c, \epsilon_\theta)$ or $(\sigma_u(\psi, \lambda), \sigma_v(\psi, \lambda), r(\psi, \lambda))$ generated by Monte Carlo method, causing hurricane track direction changing continuously. By examining 100-year hurricane simulation with 1321 synthetic hurricane tracks, there are total 8 hurricane veering cases, thus the associated probability is roughly around 0.6% (see Fig. 7).

4. Hurricane intensity modeling

Unlike hurricane trajectory tracking, described in the previous subsection, hurricane intensity (hurricane eye pressure deficit) is difficult to predict since it results from heat exchange and interaction between sea water and surrounding air. From the standpoint of civil engineering design, it is however plausible to examine the hurricane intensity from a statistical and risk perspective regardless of actual physical dynamics.

As indicated in [4], Eq. (2) alone cannot accurately predict hurricane intensity. As a result, additional parameters are usually necessary to adjust the hurricane intensity computations [20,4]. In this paper an approach based on auto-regressive (AR) model formulation is proposed. The idea is presented in Eq. (11) below. An AR(2) process, with ϵ_I error term, is used to reproduce the stochastic properties of hurricane intensity and its variation over sea surface at time step i; this yields:

$$\Delta I_i = c_0 + \sum_{j=1}^{2} \phi_j \Delta I_{i-j} + c_1 T_{s,i} + \epsilon_I \tag{11}$$

The calibration of the coefficients in Eq. (11) is obtained from standard Yule–Walker equations. However, a preliminary regression analysis of T_s is performed to determine the c_0 and c_1 by precluding the SST effects from hurricane intensity. The adjusted hurricane intensity is

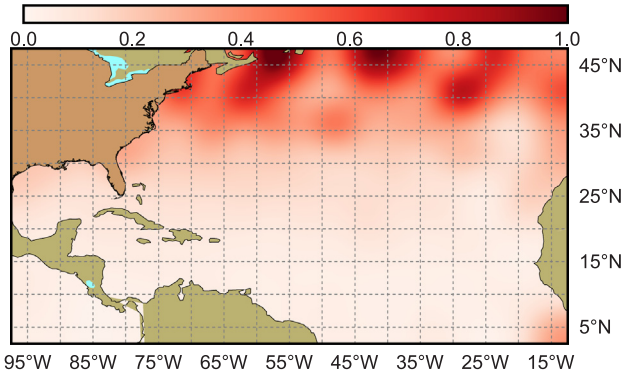

(a) $\sigma_u(\psi, \lambda)$

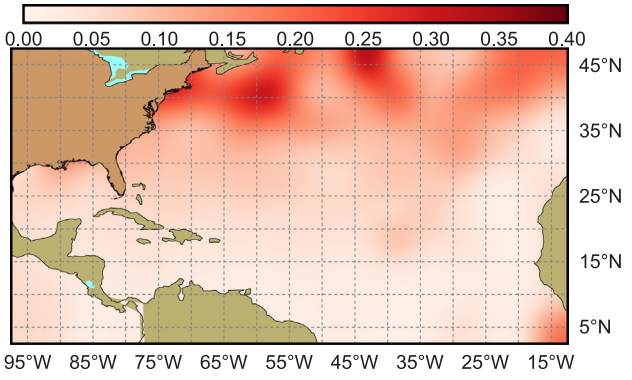

(b) $\sigma_v(\psi, \lambda)$

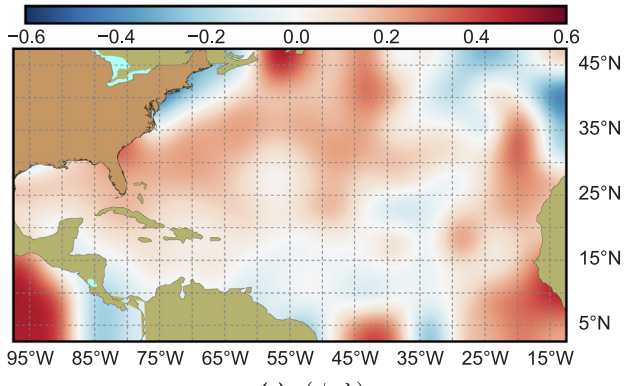

(c) $r(\psi, \lambda)$

Fig. 5. Spatially-dependent hurricane track model *diffusion* coefficients.

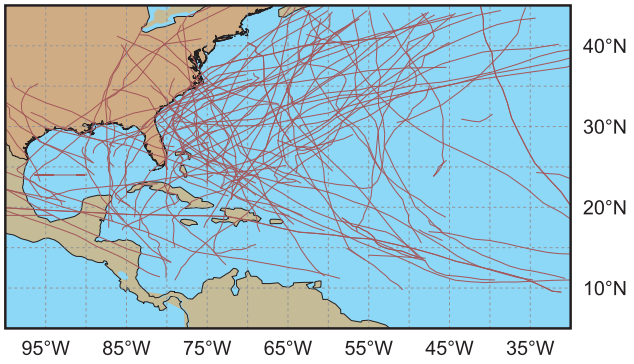

Fig. 6. Synthetic hurricanes tracks.

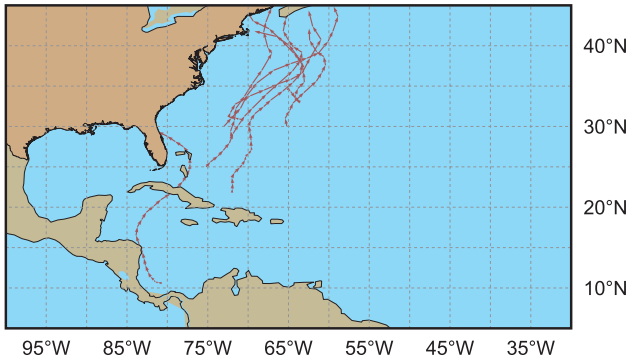

Fig. 7. 8 hurricane veering cases among 100 year simulation.

defined as $\Delta I_i' = \Delta I_i - c_0 - c_1 T_{s,i}$, and Eq. (11) is modified to a standard AR(2) model, enabling the estimation of the ϕ_j parameters.

$$\Delta I_i' = \sum_{j=1}^{2} \phi_j \Delta I_{i-j}' + \epsilon_I. \tag{12}$$

By precluding the SST effects from hurricane intensity, the intensity model in Eq. (12) can incorporate possible climate change caused by SST increasing in a projected warming climate. However, it should be admitted that climate change can affect hurricane intensity, as well as translation, in many aspects. [21,22] showed that hurricane intensity depends on many environmental variables, such as deep-layer mean vertical shear and mid-level relative humidity besides SST. [23] pointed out that hurricane genesis are affected by relative humidity, vertical shear and absolute vorticity. [6] simulated the hurricane tracks through a Markov-Chain model, which includes the veering wind effects on hurricane paths. Therefore, the hurricane patterns modeled from historic records may significantly change under climate change effect, because the environmental variables mentioned above may also change simultaneously, which exceed the capacity of the proposed model in this study.

Fig. 8 presents the normalized temporal auto-correlation (Yule–Walker equations) of the adjusted hurricane intensity time series for all historical hurricanes, which have entered the grid cell (80–75°W, 25–30°N).

Similar to the hurricane tracks, the hurricane intensity coefficients in Eq. (11) are found through the historical hurricane intensity changes recorded in each 5° × 5° grid cell and assigned to the cell center. A two-dimensional interpolation is used to determine the value of the coefficients at other locations besides cell centers.

Fig. 9 illustrates an example of 1000 synthetic simulations of hurricane pressures, traveling along the same trajectory as Hurricane Andrew (1992). The actual pressure deficit of Hurricane Andrew is plotted as a thick solid line in Fig. 9. It is noted that hurricane intensity decays

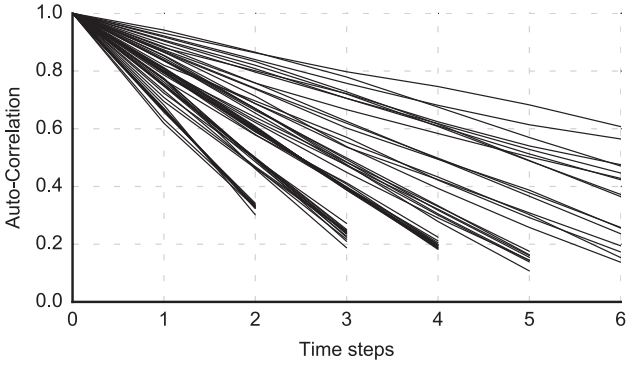

Fig. 8. Normalized auto-correlation of hurricane intensity traveling through the grid cell (80–75°W, 25–30°N).

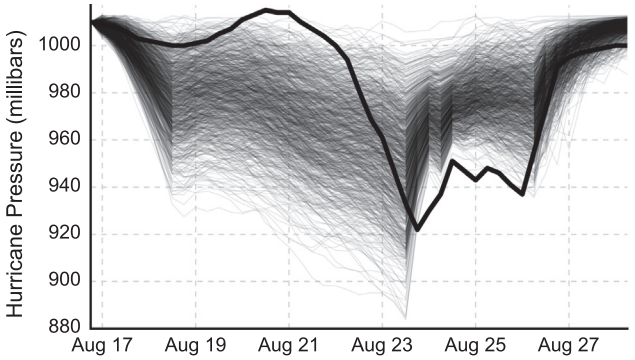

Fig. 9. 1000 simulations of hurricane central pressures along the trajectory of Hurricane Andrew.

(i.e., central pressure slightly increases) on August 24, 1992 as the storm crosses the Florida peninsula; a second hurricane intensity decay stage is also present after August 26 (larger central pressure increment) as the storm makes final landfall along the coast of the Gulf of Mexico.

After combining the hurricane track simulation model in Section 3 and the hurricane intensity model in Section 4, hurricane activities in the North Atlantic Ocean can be replicated and predicted by Monte Carlo sampling. The initial "birthplace" of a hurricane is randomly sampled from the HurDat Database, shown in Fig. 10. The overall Hurricane frequency in the North Atlantic Ocean basin is represented as a Negative Binomial process [4]. After landing, the hurricane intensity decay model presented in Section 2.2 is adopted in this study.

5. Model validation

In order to verify the adequacy of the proposed hurricane simulation method, one century (100 years) of hurricane activities are numerically generated. Results are compared against the HurDat records. The comparison method is adapted from [4]. The mean and standard deviations of the simulated vs. real hurricanes are cross-examined as they land in the proximity of the mileposts (MPs) [4], shown in Fig. 11, along the US Atlantic coastline. The MP numbering starts from the USA-Mexico border and progressively increases; distance between two consecutive MPs is 500 km.

Fig. 12a) summarizes hurricane landing frequency at various MPs. Adequate correspondence can be observed, confirming that synthetic hurricane frequency and landing position are compatible with historical records. Figs. 12b) and c) illustrate the mean and RMS values of the hurricane center translation speeds in the latitude and longitude directions at all MPs. An overall agreement of both mean and RMS values can be noted in all the panels of Fig. 12. Although some differences exist in the RMS values between simulated hurricane translation speed and the HurDat records, the proposed hurricane simulation algorithm is adequate and sufficiently accurate. The large RMS deviation between historic longitude speeds and simulated results may be due to the coarse

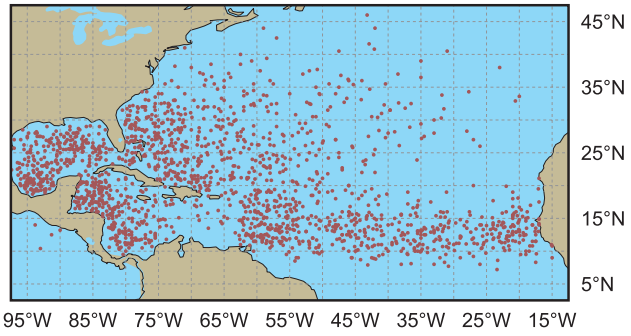

Fig. 10. Hurricane genesis locations in the North Atlantic Ocean.

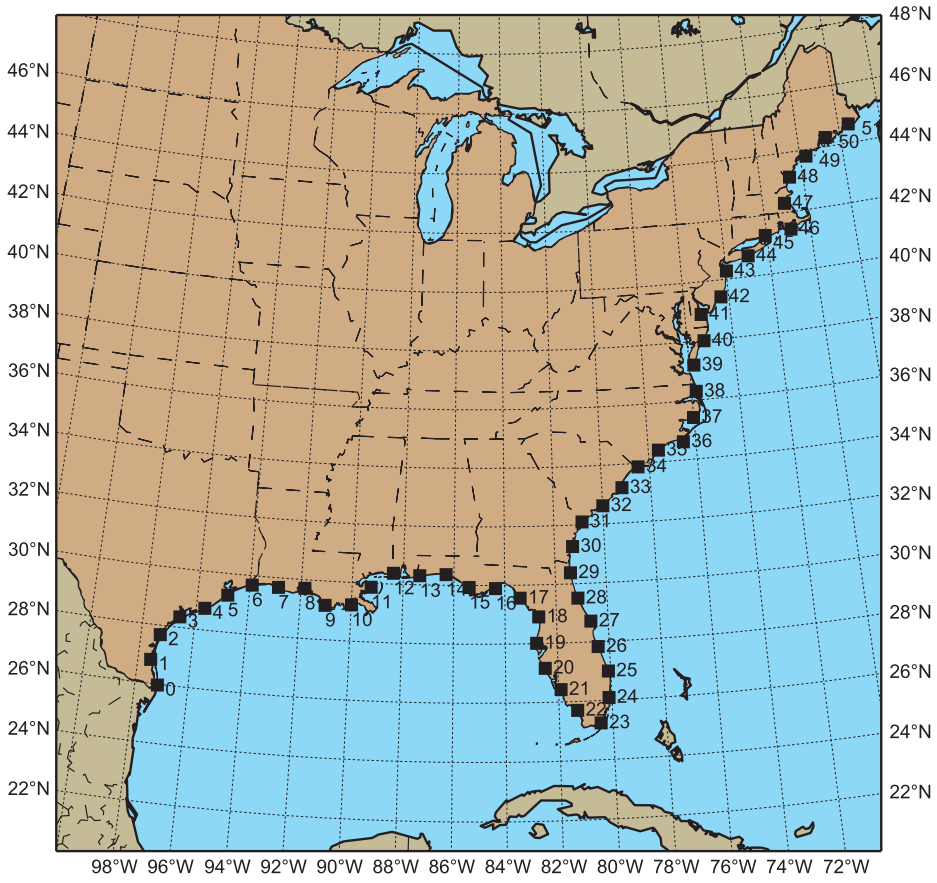

Fig. 11. Locations of MPs along the US Atlantic coastline.

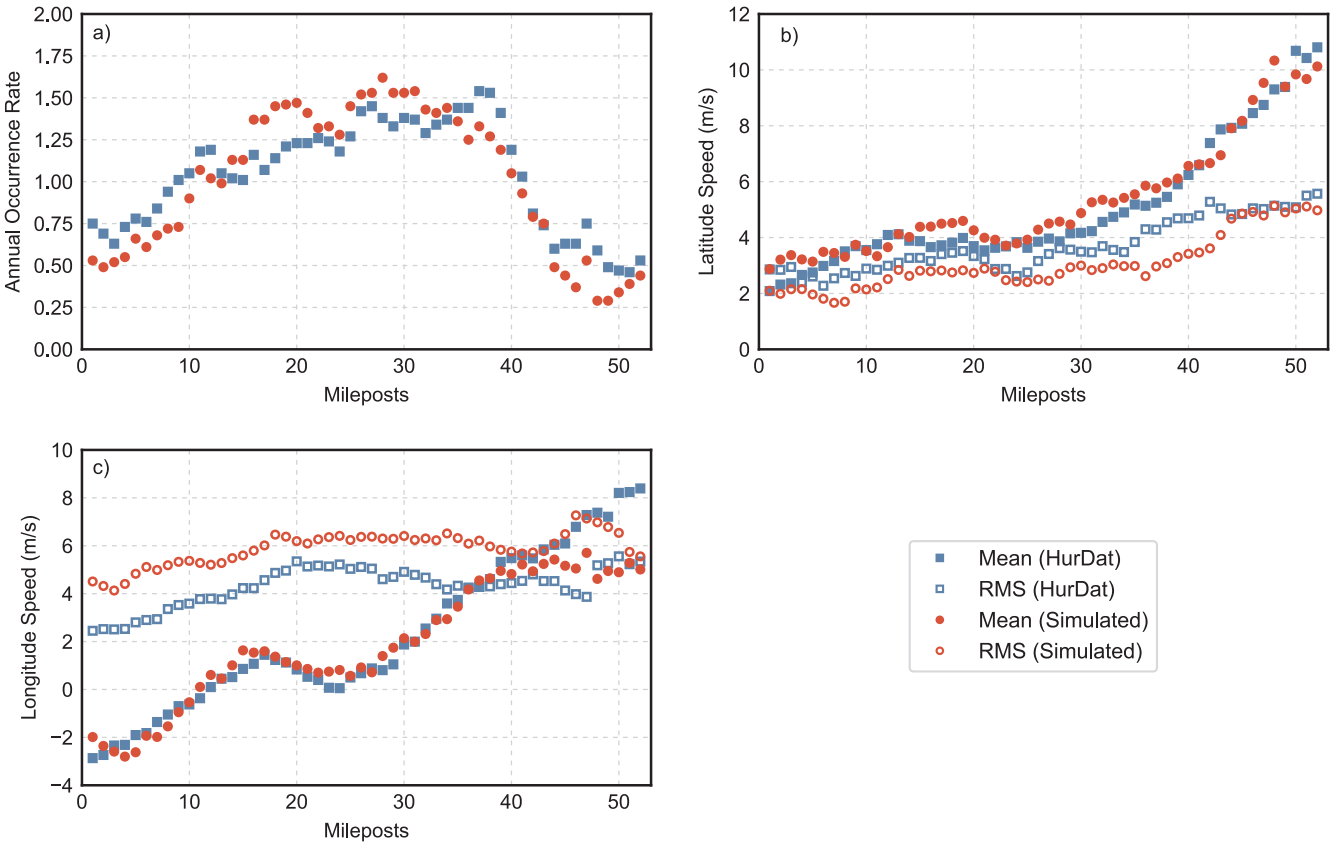

Fig. 12. Validation of simulated hurricane occurrence rate and translation speeds at landfall.

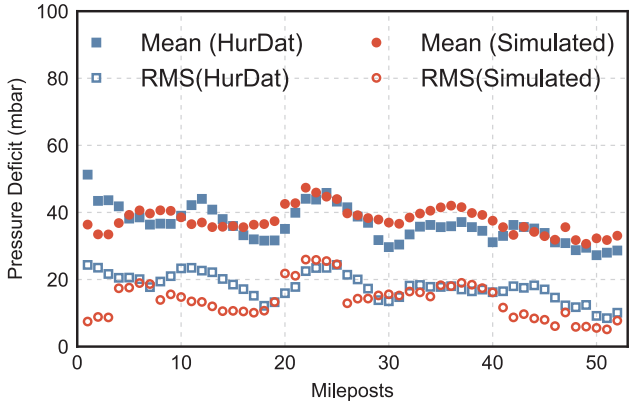

Fig. 13. Validation of simulated hurricane central pressures at landfall: mean values and standard deviations.

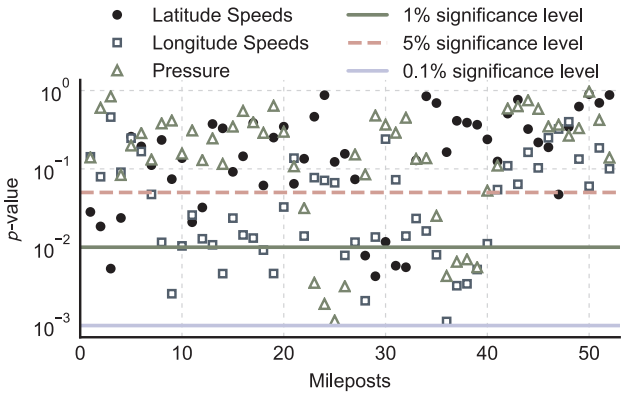

Fig. 14. Validation of simulated hurricane latitude, longitude speeds and central pressures at landfall: p-values from Kolmogorov–Smirnov statistical tests.

grid size ($5^\circ \times 5^\circ$); a refined grid will be implemented in future study.

Similarly, Fig. 13 compares the central pressure of major hurricanes (pressure deficit $\Delta p \geq 30$ MPa) at various MPS; the figure confirms that simulated hurricane intensity matches with the historical hurricane records along the US eastern coastline.

For validation purposes, the Kolmogorov–Smirnov goodness-of-fit test [24] is performed at each MP to compare the simulated hurricane translation speed and central pressure results against the HurDat data set. The p-values from the test results are illustrated in Fig. 14. The three statistical tests, conducted on latitude and longitude translation

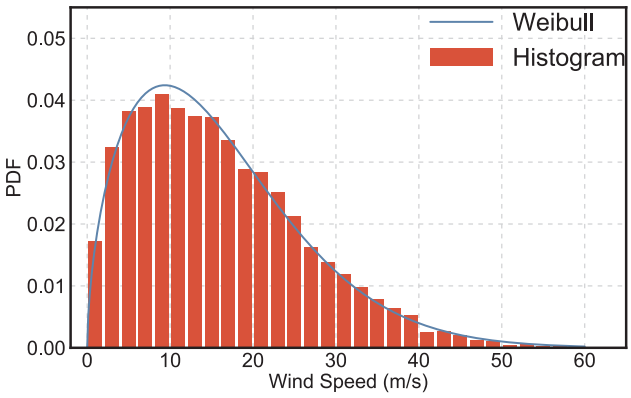

(a) Distribution of wind speed (m/s): empirical histogram and Weibull model

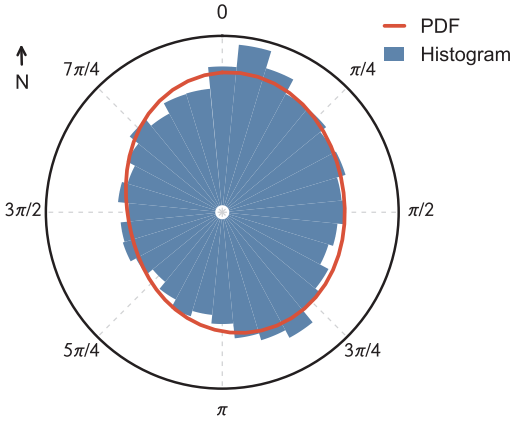

(b) Reference wind direction θ (rad)

Fig. 16. Distribution of hurricane reference gradient wind speed (m/s) and angular distributions of hurricane reference wind direction θ at Miami, FL, USA: empirical histograms and PDF models.

speeds and pressure deficit at landfall on all MPs, pass at the 0.001 significance level. Small differences are reasonable for the purposes of this study, also because both simulated and real hurricanes are random processes and the HurDat hurricane information was often incomplete during the early stages of the project. Most disparities can be found from MP 20 to MP 40, which may be influenced by the complex coastline configuration around the Florida peninsula. It is possible to

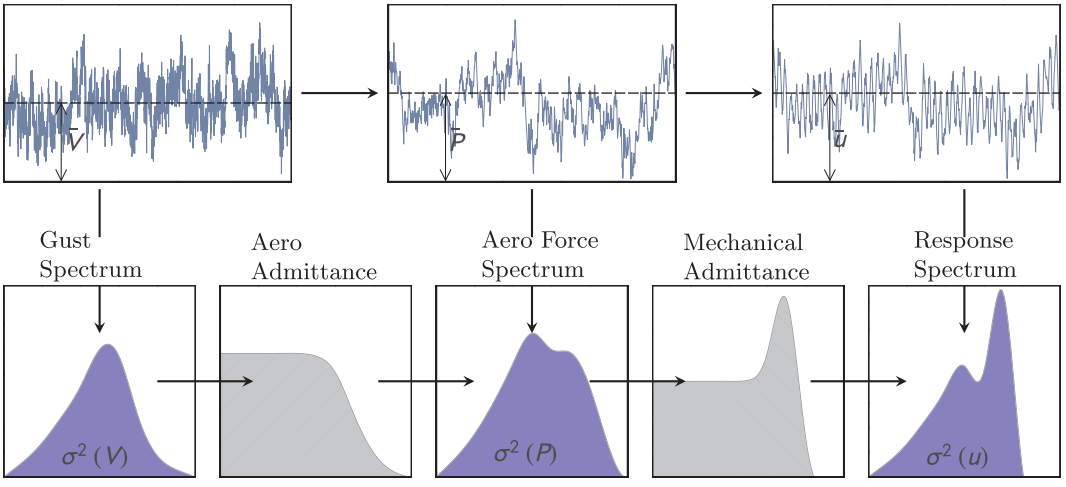

Fig. 15. Davenport Chain [28].

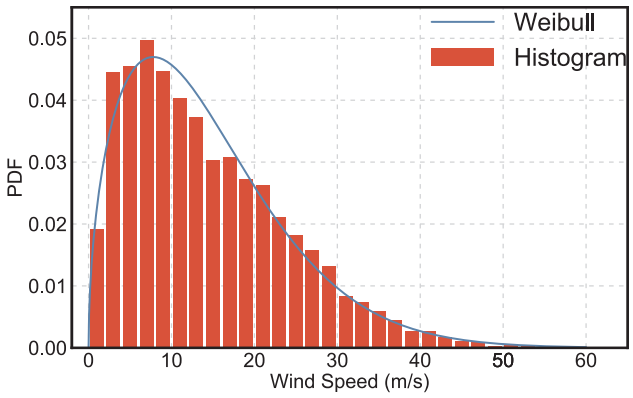

(a) Distribution of wind speed (m/s): histogram and Weibull model

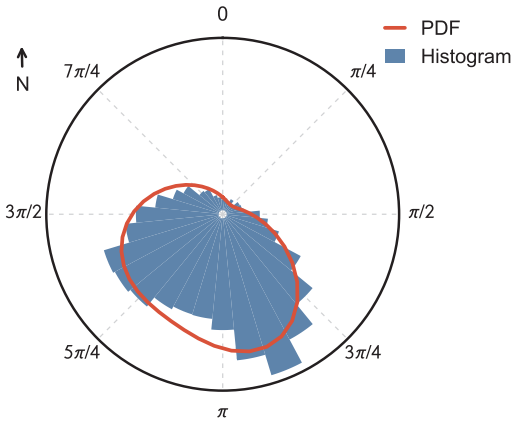

(b) Reference wind direction θ (rad)

Fig. 17. Distribution of hurricane reference gradient wind speed (m/s) and angular distribution of hurricane reference wind direction θ at Tampa, FL, USA: empirical histograms and PDF models.

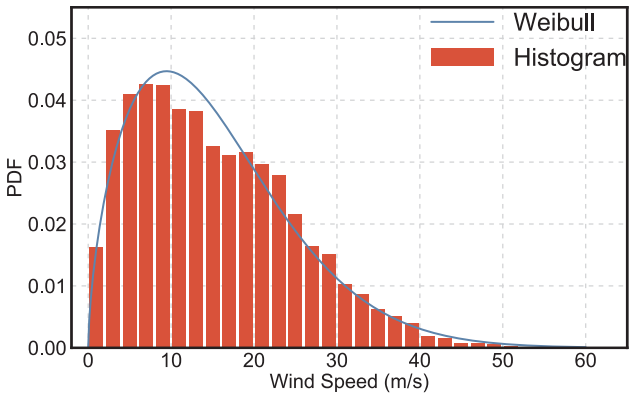

(a) Distribution of wind speed (m/s): histogram and Weibull model

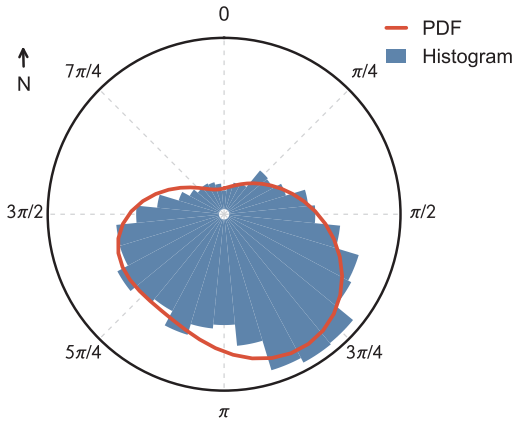

(b) Reference wind direction θ (rad)

Fig. 18. Distribution of hurricane reference gradient wind speed (m/s) and angular distribution of hurricane reference wind direction θ at New Orleans, LA, USA: empirical histograms and PDF models.

improve the simulation accuracy by refining the grid and cell size during the calibration of the coefficients in Eq. (9). It should also be noted that the hurricane simulation cannot perform as accurately as Vickery's model since additional calibration of extra regional coefficients is necessary according to [4].

6. Application of hurricane simulation results

One of the most important applications of hurricane simulation results is related to PBWE. As illustrated in the Davenport Chain, shown in Fig. 15, analysis of wind speeds from local wind climate is always the first step of wind engineering design. Hurricane simulation results can provide complete probabilistic description of wind speed distribution instead of design wind speed values at selected, pre-fixed return periods (typical of the prescriptive design philosophy). Probability distributions are necessary for structural design to meet special performance requirements and flexible demands [25–27].

In this study, 20,000 years of hurricane simulation results are repeated; results are extracted for Miami, Florida (25.78° N, 80.21° W) as an example. During the 20,000-year simulation, there are 13687 years when hurricane activity is recorded within the influence region 300 km around Miami, yielding as annual average hurricane landing probability $P(\mathrm{Hl}) = 13687/20000 = 0.684$. From each year, in which hurricane landing is numerically predicted, the maximum gradient wind speeds and the associated wind directions are extracted. Results are plotted in Fig. 16. The hurricane gradient wind speeds are calculated for each hurricane according to Georgiou's wind field model, demonstrated in Section 2.3. In Fig. 16a, the histogram of the wind speed annual maxima and corresponding probability density function (PDF) are presented. The Weibull distribution model can adequately replicate the distribution of hurricane wind speeds [29,2]. Fig. 16b illustrates the distribution of hurricane wind direction and the corresponding PDF model, derived as a mixture of von Mises angular distribution models [30].

The probability distributions of wind speeds can readily be derived for various locations along the US eastern coastline, such as Tampa, Florida in Fig. 17, New Orleans, Louisiana in Fig. 18, Norfolk, Virginia in Fig. 19 and New York, New York in Fig. 20. This information can later be used within the Davenport Chain to evaluate the structural performance under random wind load excitation.

Hurricane simulation results can be employed to estimate the design wind speeds associated with various return periods in hurricane-prone regions as follows:

$$\frac{1}{1+\overline{N}} = [1 - F_V(v)]P(\mathrm{Hl}) \tag{13}$$

In the previous equation $\overline{N}$ is the return period in years, $F_V(v)$ is the cumulative distribution function (CDF) of hurricane wind speed v within the influence region of a specific location, conditional on the landing of at least one hurricane in that year. $P(\mathrm{Hl})$ is the annual probability of at least one hurricane having landed around the given area.

According to Eq. (13) and the simulation results, the wind speeds associated with 7 different return periods

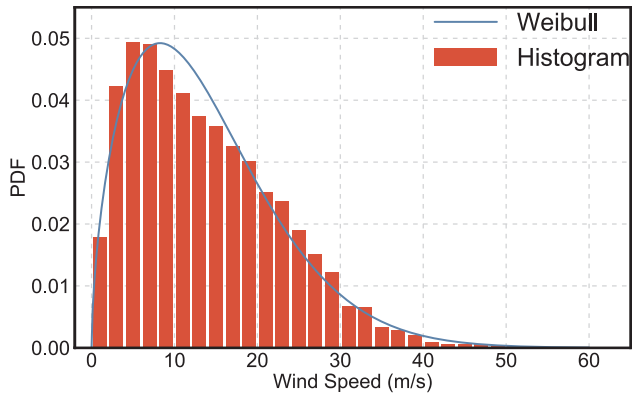

(a) Distribution of wind speed (m/s): histogram and Weibull model

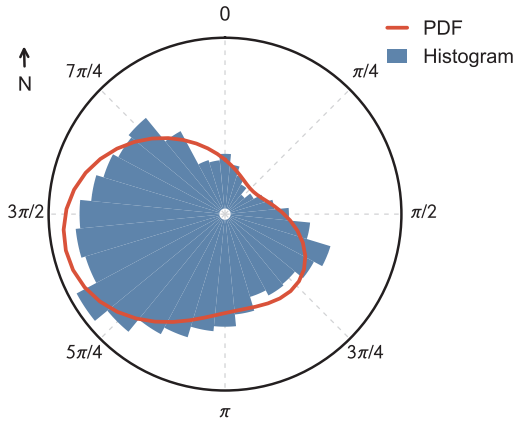

(b) Reference wind direction θ (rad)

Fig. 19. Distribution of hurricane reference gradient wind speed (m/s) and angular distribution of hurricane reference wind direction θ at Norfolk, VA, USA: empirical histograms and PDF models.

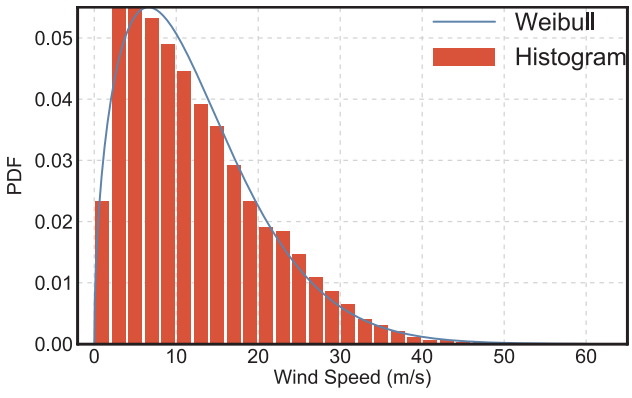

(a) Distribution of wind speed (m/s): histogram and Weibull model

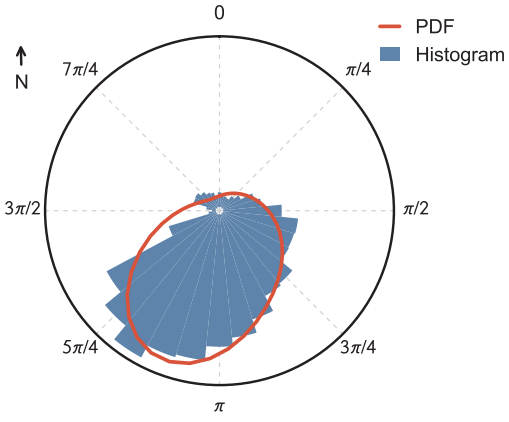

(b) Reference wind direction θ (rad)

Fig. 20. Distribution of hurricane reference gradient wind speed (m/s) and angular distribution of hurricane reference wind direction θ at New York, NY, USA: empirical histograms and PDF models.

$\overline{N}$ = 10, 25, 50, 100, 300, 700, 1700 years at Miami, Tampa, New Orleans, Norfolk and New York are presented in Table 3. The gradient-to-surface wind speed conversion factor is taken from [32].

The design wind speeds suggested by ASCE-7 [31] are also displayed in Table 3. For high latitude areas, such as Norfolk and New York, the hurricane simulated wind speeds for short return periods ($\overline{N}$ = 10, 25 years) are smaller than the ASCE-7 design wind speeds, because other, non-hurricane wind events predominantly contribute to the PDF as opposed to hurricanes. In the case of intermediate return periods ($50 \leqslant \overline{N} \leq 100$ years), the simulated results are usually compatible with ASCE-7 provisions at both high and low latitudes. However, for the longer return periods ($300 \leqslant \overline{N} \leq 1700$ years), the simulated results are generally larger than the ASCE-7 results. One plausible reason for this difference is that, for such small-probability events, there are very few valid hurricane occurrences. Therefore, the design wind speeds for longer return periods largely depends on the selection of the distribution model. The one proposed in this study (Weibull distribution) is likely different from the model employed by ASCE-7. Nevertheless, hurricane contribute significantly to the extreme wind levels along the US coastline [33], and additional studies should be devoted to the examination of hurricane wind speed simulation methods and distribution probability models.

7. Conclusions

In this study, a new synthetic hurricane simulation algorithm is presented. The method uses a two-dimensional correlated Brownian motion process to model the hurricane tracks in Cartesian coordinates. In contrast with existing data-driven hurricane simulation approaches, calibration of fewer model coefficients is needed. Furthermore, separation of the model coefficients into two sets, depending on hurricane heading (westward or eastward), is avoided. An auto-regressive model is employed to describe hurricane intensity (central pressure deficit), preserving information from previous simulation steps rather than directly computing the intensity from an empirical linear equation. The proposed algorithm reduces the complexity of the simulation process. The comparison with historical hurricane records suggests that the proposed method is a valid alternative to the current hurricane simulation approach [4]. At last, application of hurricane simulation results is discussed in the context of performance-based wind engineering; the synthetically-generated hurricane wind speeds at hurricane-prone region associated with different return periods are compared to ASCE-7 design wind speeds to ensure the structural engineering applicability of the proposed hurricane simulations.

Declaration of Competing Interest

The authors declared that there is no conflict of interest.

Acknowledgments

This material is based upon work supported in part by the National Science Foundation (NSF) of the United States of America under CAREER Award CMMI-0844977 in 2009–2014. The support of MathWorks Inc., Natick, Massachusetts, USA through a micro-grant awarded by Northeastern University and Professor Miriam Leeser in

Table 3
Estimated 10-min hurricane wind speeds (m/s) at 10 m above ground in open terrain at selected locations along US coastline as a function of return period $\overline{N}$.

Location/Return period [years]	Miami, FL		Tampa, FL		New Orleans, LA		Norfolk, VA		New York, NY	
	*	#	*	#	*	#	*	#	*	#
$\overline{N}$ = 10	**24.2**	24.1	**21.3**	18.4	**21.8**	21.0	**21.2**	17.1	**20.2**	14.1
$\overline{N}$ = 25	**30.4**	32.2	**25.6**	24.6	**25.9**	26.8	**23.2**	21.6	**22.4**	18.6
$\overline{N}$ = 50	**34.7**	34.5	**28.5**	29.0	**29.1**	30.9	**25.3**	24.8	**24.5**	21.7
$\overline{N}$ = 100	**37.7**	38.6	**31.5**	33.0	**31.8**	34.7	**26.6**	27.8	**25.9**	24.7
$\overline{N}$ = 300	**42.3**	44.7	**35.3**	39.1	**35.8**	40.3	**29.4**	32.3	**28.8**	29.2
$\overline{N}$ = 700	**45.5**	49.1	**38.0**	43.5	**38.8**	44.4	**32.0**	35.5	**31.0**	32.4
$\overline{N}$ = 1700	**49.0**	53.5	**40.4**	47.8	**41.2**	48.4	**34.7**	38.7	**33.9**	35.6

Case ∗: reference value derived from ASCE 7 [31].
Case #: simulated design wind speeds.

2015 is also gratefully acknowledged. Finally, the sponsorship of Shanghai Pujiang Program (No. 19PJ1409800) is acknowledged. Any opinions, findings and conclusions or recommendations are those of the authors and do not necessarily reflect the views of either the NSF or any other sponsor.

References

[1] Georgiou PN. Design wind speeds in tropical cyclone-prone regions. Ph.D. Dissertation. London, Ontario, Canada: University of Western Ontario; 1986.
[2] Simiu E, Scanlan RH. Wind effects on structures: fundamentals and applications to design. 3rd ed. New Jersey, USA: John Wiley & Sons; 1996.
[3] Simiu E, Yeo D. Wind effects on structures: modern structural design for wind. 4th ed. New Jersey, USA: Wiley-Blackwell; 2019.
[4] Vickery P, Skerlj P, Twisdale L. Simulation of hurricane risk in the U.S. using empirical track model. J Struct Eng 2000;126(10):1222–37.
[5] Vickery PJ, Skerlj P, Steckley A, Twisdale L. Hurricane wind field model for use in hurricane simulations. J Struct Eng 2000;126(10):1203–21.
[6] Emanuel K, Ravela S, Vivant E, Risi C. A statistical deterministic approach to hurricane risk assessment. Bull Am Meteorol Soc 2006;87(3):299–314.
[7] Lee KH, Rosowsky DV. Synthetic hurricane wind speed records: development of a database for hazard analyses and risk studies. Natural Hazards Rev 2007;8(2):23–34.
[8] Powell M, Soukup G, Cocke S, Gulati S, Morisseau-Leroy N, Hamid S, et al. State of Florida hurricane loss projection model: Atmospheric science component. J Wind Eng Ind Aerodyn 2005;93(8):651–74.
[9] Vickery PJ, Wadhera D, Twisdale Jr LA, Lavelle FM. US hurricane wind speed risk and uncertainty. J Struct Eng (ASCE) 2009;135(3):301–20.
[10] Vickery PJ, Wadhera D, Galsworthy J, Peterka JA, Irwin PA, Griffis LA. Ultimate wind load design gust wind speeds in the United States for use in ASCE-7. J Struct Eng (ASCE) 2009;136(5):613–25.
[11] Hong HP, Li SH, Duan ZD. Typhoon wind hazard estimation and mapping for coastal region in mainland china. Nat Hazards Rev 2016;17(2):04016001.
[12] Lee JY, Ellingwood BR. Intergenerational risk-informed decision framework for civil infrastructure. In: Deodatis G, Ellingwood BR, Frangopol DM, editors. Safety, reliability, risk and life-cycle performance of structures and infrastructures. Balkema: CRC Press; 2014. p. 3369–74.
[13] Liu F. Projections of future US design wind speeds due to climate change for estimating hurricane losses. Ph.D. Dissertation. Clemson, South Carolina: Clemson University; 2014.
[14] Cui W, Caracoglia L. Exploring hurricane wind speed along US Atlantic coast in warming climate and effects on predictions of structural damage and intervention costs. Eng Struct 2016;122:209–25.
[15] Darling R. Estimating probabilities of hurricane wind speeds using a large-scale empirical model. J Clim 1991;4(10):1035–46.
[16] Vickery PJ, Twisdale LA. Wind-field and filling models for hurricane wind-speed predictions. J Struct Eng 1995;121(11):1700–9.
[17] Vickery PJ. Simple empirical models for estimating the increase in the central pressure of tropical cyclones after landfall along the coastline of the United States. J Appl Meteorol 2005;44(12):1807–26.
[18] Mudd L, Wang Y, Letchford C, Rosowsky D. Assessing climate change impact on the U.S. east coast hurricane hazard: temperature, frequency, and track. Nat Hazards Rev 2014;15(3):04014001.
[19] Grigoriu M. Stochastic calculus: applications in science and engineering. Boston, MA, USA: Birkhäuser; 2002.
[20] Li S, Hong H. Observations on a hurricane wind hazard model used to map extreme hurricane wind speed. J Struct Eng 2014.
[21] Lee CY, Tippett MK, Sobel AH, Camargo SJ. Autoregressive modeling for tropical cyclone intensity climatology. J Clim 2016;29(21):7815–30.
[22] Lin N, Jing R, Wang Y, Yonekura E, Fan J, Xue L. A statistical investigation of the dependence of tropical cyclone intensity change on the surrounding environment. Mon Weather Rev 2017;145(7):2813–31.
[23] Lee CY, Tippett MK, Sobel AH, Camargo SJ. An environmentally forced tropical cyclone hazard model. J Adv Model Earth Syst 2018;10(1):223–41.
[24] Massey Jr FJ. The Kolmogorov-Smirnov test for goodness of fit. J Am Stat Assoc 1951;46(253):68–78.
[25] Cui W, Caracoglia L. Simulation and analysis of intervention costs due to wind-induced damage on tall buildings. Eng Struct 2015;87:183–97.
[26] van de Lindt J, Dao T. Performance-based wind engineering for wood-frame buildings. J Struct Eng 2009;135(2):169–77.
[27] Ciampoli M, Petrini F. Performance-based Aeolian risk assessment and reduction for tall buildings. Probab Eng Mech 2012;28:75–84.
[28] Isyumov N, Alan G. Davenport's mark on wind engineering. J Wind Eng Ind Aerodyn 2012;104:12–24.
[29] Cui W, Caracoglia L. A unified framework for performance-based wind engineering of tall buildings in hurricane-prone regions based on lifetime intervention-cost estimation. Struct Saf 2018;73:75–86.
[30] Johnson RA, Wehrly TE. Some angular-linear distributions and related regression models. J Am Stat Assoc 1978;73(363):602–6.
[31] ASCE. Minimum design loads for building and other structures (ASCE 7-16); 2016.
[32] Batts ME, Simiu E, Russell LR. Hurricane wind speeds in the United States. J Struct Div 1980;106(10):2001–16.
[33] Yeo D, Lin N, Simiu E. Estimation of hurricane wind speed probabilities: Application to New York City and other coastal locations. J Struct Eng 2013;140(6):04014017.